doi: 10.15407/ujpe61.02.0134

I.S. BZOVSKA, I.M. MRYGLOD

Institute for Condensed Matter Physics, Nat. Acad. of Sci. of Ukraine
(1, Svientsitskoho Str., Lviv 79011, Ukraine; e-mail: iryna@icmp.lviv.ua)

PACS 82.40.Bj, 82.45.Jn

SURFACE PATTERNS IN CATALYTIC CARBON MONOXIDE OXIDATION REACTION

The mechanism of spatio-temporal pattern formation at the catalytic oxidation of carbon monoxide on the Pt(110) surface has been studied. The surface may contain structurally different areas, which are formed in the course of the CO-induced transition from the reconstructed 1×2 *phase to the* 1×1 *(bulk) one. Temporal and spatial instabilities in the system are analyzed, by using the methods of the linear theory of stability and numerical simulations. Fragments of spatio-temporal structures of the oxygen coverage together with fragments of the surface* 1×1 *structure are shown to emerge on the inhomogeneous surface at certain system parameters. The distribution of the carbon monoxide coverage is found to be almost homogeneous in space and independent of the surface geometry.*

K e y w o r d s: catalytic oxidation reaction, reaction-diffusion model, spatio-temporal patterns, Hopf bifurcation.

1. Introduction

The self-organization processes, i.e. the spontaneous emergence of an order, in reaction-diffusion systems have been drawing a considerable attention of chemists, physicists, and biologists for a long time. Modern experimental techniques of surface research, in particular, photoemission electron microscopy, demonstrate a variety of phenomena such as the propagation of reaction fronts, standing waves, spirals, chemical turbulence, and so on [1–4].

The emergence of non-equilibrium structures in such media is associated with the interaction between nonlinear local transformations characterized by a positive feedback (autocatalysis, surface phase transitions, and so forth) and transport processes (diffusion) that spatially connect the system. Two widely known chemical systems corresponding to those criteria are the autocatalytic Belousov–Zhabotinskii reaction [5, 6] and the reaction of carbon monoxide oxidation on a platinum surface [7–10]. These reactions are inherent in systems that are far from the thermodynamic equilibrium. They occur, when a system exchanges particles and energy with the environment. The orientation of the catalyst surface in such a system has a crucial influence on the emergence of oscillations and surface patterns. A pure Pt surface is reconstructed and presents a 1×2 structure. If its coverage with adsorbed CO molecules exceeds a certain critical value, the surface returns to the bulk configuration, the 1×1 structure. As a result, the Pt(110) surface becomes inhomogeneous and contains areas with different atomic orderings (1×2 or 1×1). The dependence of the oxygen adsorption probability on structural surface modifications gives rise to the excitation of spatio-temporal oscillations on the surface.

The research of instabilities in time and space on the basis of reaction-diffusion models for such reactions enables some general properties of rather a wide class of non-equilibrium systems to be revealed [11]. Knowing the mechanisms giving rise to the emergence and the destruction of spatio-temporal structures and having found ways to control them, it would be possible to create new promising devices to process information, to develop methods aimed at increasing the efficiency in chemical industry, and so on.

In this work, the mechanism of spatio-temporal surface pattern formation has been studied in the framework of the reaction-diffusion model for the reaction of carbon monoxide oxidation on the Pt(110) surface. The analysis of instabilities in time and space is carried on, by using the methods of the linear theory of stability and numerical simulations. It will be shown that, at the certain values of parameters, there emerge real patterns in the system, which are predicted by the linear analysis and are similar to those observed experimentally.

2. Reaction Model and Analysis of Stability

Let us consider a model for the reaction of catalytic oxidation of carbon monoxide, in which the diffusion of CO molecules on the Pt(110) surface – processes of surface reconstruction are typical of it – is made allowance for. For this purpose, the diffusion term is included into the system of kinetic differential equations describing the dynamic behavior of the model [12]. The new term takes into account the diffusion of carbon monoxide molecules on the catalyst surface [13]. As a result, we obtain

$$\begin{aligned}
&\frac{\mathrm{d}\theta_{\mathrm{CO}}}{\mathrm{d}\tau} = D\triangle\theta_{\mathrm{CO}} + p_{\mathrm{CO}}k_{\mathrm{CO}}s_{\mathrm{CO}}(1-\theta_{\mathrm{CO}}^{q}) - \\
&- d\theta_{\mathrm{CO}} - k_r\theta_{\mathrm{CO}}\theta_{\mathrm{O}}, \\
&\frac{\mathrm{d}\theta_{\mathrm{O}}}{\mathrm{d}\tau} = p_{\mathrm{O}_2}k_{\mathrm{O}}(s_{\mathrm{O}}^{1\times1}\theta_{1\times1} + s_{\mathrm{O}}^{1\times2}(1-\theta_{1\times1}))\times \\
&\times(1-\theta_{\mathrm{CO}}-\theta_{\mathrm{O}})^2 - k_r\theta_{\mathrm{CO}}\theta_{\mathrm{O}}, \\
&\frac{\mathrm{d}\theta_{1\times1}}{\mathrm{d}\tau} = k_5\left(\left[1+\exp\left(\frac{u_0-\theta_{\mathrm{CO}}}{\delta u}\right)\right]^{-1} - \theta_{1\times1}\right).
\end{aligned} \tag{1}$$

The explanation of parameters of the equation and their values used in further calculations are tabulated in Table (see work [13]). The first equation of system (1) describes the variation of the adsorbed CO amount with regard for the chemical reaction with the adsorbed oxygen, CO desorption with the desorption constant d, and CO diffusion. The first term in the second equation of system (1) describes the dissociative oxygen adsorption, and the second one corresponds to variations due to the CO oxidation. The last equation in system (1) is a model kinetic equation that describes the surface transformation of non-reconstructed 1×1 structure. The multiplier $\left[1+\exp\left(\frac{u_0-\theta_{\mathrm{CO}}}{\delta u}\right)\right]^{-1}$ in it is a nondecreasing smooth function of θ_{CO} within the segment [0,1], which makes it possible to describe the transition from the reconstructed surface with 1×2 structure to that with 1×1 structure depending on the CO coverage. This model involves also the precursor mechanism for the CO adsorption kinetics by means of the exponent $q=3$ on the right-hand side of the first equation in system (1). This account makes the model more realistic, because the adsorption suppression for CO and O_2 is asymmetric: adsorbed CO blocks the oxygen adsorption more strongly.

In the terms of dimensionless variables, system (1) looks like

$$\begin{aligned}
&\frac{\mathrm{d}\theta_{\mathrm{CO}}}{\mathrm{d}t} = F_{\mathrm{CO}}(\theta_{\mathrm{CO}},\theta_{\mathrm{O}}) = \overline{D}\triangle\theta_{\mathrm{CO}} + \overline{p}_{\mathrm{CO}}(1-\theta_{\mathrm{CO}}^3) - \\
&- \overline{d}\theta_{\mathrm{CO}} - \theta_{\mathrm{CO}}\theta_{\mathrm{O}}, \\
&\frac{\mathrm{d}\theta_{\mathrm{O}}}{\mathrm{d}t} = F_{\mathrm{O}}(\theta_{\mathrm{CO}},\theta_{\mathrm{O}},\theta_{1\times1}) = \overline{p}_{\mathrm{O}_2}(1+\theta_{1\times1})\times \\
&\times(1-\theta_{\mathrm{CO}}-\theta_{\mathrm{O}})^2 - \theta_{\mathrm{CO}}\theta_{\mathrm{O}}, \\
&\frac{\mathrm{d}\theta_{1\times1}}{\mathrm{d}t} = F_{1\times1}(\theta_{\mathrm{CO}},\theta_{1\times1}) = \\
&= \overline{k}_5\left(\left[1+\exp\left(\frac{u_0-\theta_{\mathrm{CO}}}{\delta u}\right)\right]^{-1} - \theta_{1\times1}\right),
\end{aligned} \tag{2}$$

where $t = k_r\tau$ is the dimensionless time, $\overline{D} = D/k_r$ is the dimensionless diffusion coefficient for CO molecules, $\overline{p}_{\mathrm{CO}} = p_{\mathrm{CO}}k_{\mathrm{CO}}s_{\mathrm{CO}}/k_r$, $\overline{p}_{\mathrm{O}_2} = p_{\mathrm{O}_2}k_{\mathrm{O}}s_{\mathrm{O}}^{1\times2}/k_r$, $\overline{d} = d/k_r$, and $\overline{k}_5 = k_5/k_r$ are dimensionless parameters characterizing the system, and $s_{\mathrm{O}} = s_{\mathrm{O}}^{1\times1}\theta_{1\times1} + s_{\mathrm{O}}^{1\times2}(1-\theta_{1\times1}) = s_{\mathrm{O}}^{1\times2}(1+\theta_{1\times1})$, by assuming that $s_{\mathrm{O}}^{1\times1}/s_{\mathrm{O}}^{1\times2} \simeq 2$ for Pt(110).

The system of partial differential equations (2) cannot be solved analytically in the general case. Therefore, the analysis of instabilities of the system in time and space was carried out, by using the methods of the linear theory of stability and carrying out the numerical simulation. The system of equations (2) in the linear approximation for the deviations from the stationary state $\delta\theta_i(\mathbf{r},t) = \theta_i(\mathbf{r},t) - \theta_{i,s}(\mathbf{r})$ looks

Model parameters and their values used in numerical calculations

T	540 K	Temperature
p_{O_2}	9.75×10^{-5} Torr	Partial pressure of O_2
k_{CO}	4.2×10^5 $\mathrm{s^{-1}Torr^{-1}}$	Frequency of CO molecule collisions with the surface
k_{O}	7.8×10^5 $\mathrm{s^{-1}Torr^{-1}}$	Frequency of O_2 molecule collisions with the surface
d	10.21 $\mathrm{s^{-1}}$	Rate of CO molecule desorption
D	10^{-7} $\mathrm{cm^2s^{-1}}$	Rate of CO molecule diffusion
k_r	283.8 $\mathrm{s^{-1}}$	Reaction rate
s_{CO}	1	CO sticking coefficient
$s_{\mathrm{O}}^{1\times2}$	0.4	Oxygen sticking coefficient on the 1×2 phase
u_0	0.35	Parameters for the structural
δu	0.05	phase transition
k_5	1.61 $\mathrm{s^{-1}}$	Phase transition rate

like

$$\frac{\partial}{\partial t}\delta\theta_i(\mathbf{r},t) = \sum_j \left(\frac{\partial F_i}{\partial \theta_j}\right)_{\theta_k=\theta_{k,s}} \delta\theta_j(\mathbf{r},t) + \\ + \overline{D}\triangle\delta\theta_i(\mathbf{r},t), \quad i,j = \mathrm{CO},\mathrm{O},1\times 1. \tag{3}$$

The stability of the system will be analyzed, by using the method of normal modes with respect to a spatially periodic perturbation (a normal mode) with the wavelength λ. For this purpose, we make the substitution $\delta\theta_i(\mathbf{r},t) \sim \mathrm{e}^{\omega t + i\mathbf{kr}}$, where $k = 2\pi/\lambda$ is the wave number, and obtain a linear system of equations:

$$\sum_j \left[\left(\frac{\partial F_i}{\partial \theta_j}\right)_{\theta_k=\theta_{k,s}} - \overline{D}k^2\delta_{\mathrm{CO,CO}} - \omega\delta_{ij}\right]\delta\theta_j = 0, \\ i,j = \mathrm{CO},\mathrm{O},1\times 1. \tag{4}$$

To analyze its stability, we have to solve the secular equation

$$\det\left|\left|\left(\frac{\partial F_i}{\partial \theta_j}\right)_{\theta_k=\theta_{k,s}} - \overline{D}k^2\delta_{\mathrm{CO,CO}} - \omega\delta_{ij}\right|\right| = 0. \tag{5}$$

From whence, we obtain the following equation for $\omega(k)$:

$$\omega^3 + b(k)\omega^2 + c(k)\omega + d(k) = 0. \tag{6}$$

Here, the following notations are introduced:

$$b(k) = \overline{k}_5 + 3\overline{p}_{\mathrm{CO}}\theta^2_{\mathrm{CO,s}} + \overline{d} + \theta_{\mathrm{O,s}} + 2\overline{p}_{\mathrm{O}_2}\times \\ \times(1+\theta_{1\times 1,s})(1-\theta_{\mathrm{CO,s}}-\theta_{\mathrm{O,s}}) + \theta_{\mathrm{CO,s}} + \overline{D}k^2, \\ c(k) = \left(3\overline{p}_{\mathrm{CO}}\theta^2_{\mathrm{CO,s}} + \overline{d} + \theta_{\mathrm{O,s}} + \overline{D}k^2\right)\times \\ \times\left(\overline{k}_5 + 2\overline{p}_{\mathrm{O}_2}(1+\theta_{1\times 1,s})\times\right. \\ \left.\times(1-\theta_{\mathrm{CO,s}}-\theta_{\mathrm{O,s}}) + \theta_{\mathrm{CO,s}}\right) + \\ + \overline{k}_5\left(2\overline{p}_{\mathrm{O}_2}(1+\theta_{1\times 1,s})(1-\theta_{\mathrm{CO,s}}-\theta_{\mathrm{O,s}}) + \theta_{\mathrm{CO,s}}\right) - \\ - \theta_{\mathrm{CO,s}}\left(2\overline{p}_{\mathrm{O}_2}(1+\theta_{1\times 1,s})(1-\theta_{\mathrm{CO,s}}-\theta_{\mathrm{O,s}}) + \theta_{\mathrm{O,s}}\right), \\ d(k) = \overline{k}_5(3\overline{p}_{\mathrm{CO}}\theta^2_{\mathrm{CO,s}} + \overline{d} + \theta_{\mathrm{O,s}} + \overline{D}k^2)\times \\ \times(2\overline{p}_{\mathrm{O}_2}(1+\theta_{1\times 1,s})(1-\theta_{\mathrm{CO,s}}-\theta_{\mathrm{O,s}}) + \theta_{\mathrm{CO,s}}) + \\ + \overline{p}_{\mathrm{O}_2}\frac{\overline{k}_5}{\delta u}\theta_{\mathrm{CO,s}}(1-\theta_{\mathrm{CO,s}}-\theta_{\mathrm{O,s}})^2\times \\ \times\frac{\exp\left(\frac{u_0-\theta_{\mathrm{CO,s}}}{\delta u}\right)}{\left(1+\exp\left(\frac{u_0-\theta_{\mathrm{CO,s}}}{\delta u}\right)\right)^2} - \\ - \overline{k}_5\theta_{\mathrm{CO,s}}(2\overline{p}_{\mathrm{O}_2}(1+\theta_{1\times 1,s})(1-\theta_{\mathrm{CO,s}}-\theta_{\mathrm{O,s}}) + \theta_{\mathrm{O,s}}).$$

The solution of the cubic equation (6) reads

$$\omega(k) = \sqrt[3]{-\frac{q(k)}{2} + \sqrt{D(k)}} + \\ + \sqrt[3]{-\frac{q(k)}{2} - \sqrt{D(k)}} - \frac{b(k)}{3},$$

where the notations

$$q(k) = \frac{2b^3(k)}{27} - \frac{b(k)c(k)}{3} + d(k), \\ p(k) = c(k) - \frac{b^2(k)}{3}, \\ D(k) = \frac{q^2(k)}{4} + \frac{p^3(k)}{27}$$

are introduced for convenience. In the general case, the parameter $D(k)$ can be both positive and negative. If $D(k) < 0$, we have a complex number under the cubic root. The cubic roots of the complex number $z = a + bi$ equal

$$\sqrt[3]{z} = \sqrt[3]{|z|}\left(\cos\frac{\varphi+2n\pi}{3} + i\sin\frac{\varphi+2n\pi}{3}\right), \\ n = 0,1,2. \\ |z| = \sqrt{a^2+b^2}, \quad \varphi = \operatorname{arctg}\frac{b}{a}.$$

In this case, the dispersion relation contains the real and imaginary parts, i.e. $\omega(k) = \operatorname{Re}\omega(k) + i\operatorname{Im}\omega(k)$, and

$$\omega_n(k) = 2\sqrt[6]{\frac{q^2(k)}{4} + |D(k)|}\cos\frac{\operatorname{arctg}\frac{2\sqrt{|D(k)|}}{q(k)}}{3}\times \\ \times\left(\cos\frac{2n\pi}{3} + i\sin\frac{2n\pi}{3}\right) - \frac{b(k)}{3}, \qquad n = 0,1,2. \tag{7}$$

The quantity

$$\operatorname{Re}\omega_n(k) = 2\sqrt[6]{\frac{q^2(k)}{4} + |D(k)|}\cos\frac{\operatorname{arctg}\frac{2\sqrt{|D(k)|}}{q(k)}}{3}\times \\ \times\cos\frac{2n\pi}{3} - \frac{b(k)}{3} \tag{8}$$

describes the stability of the solutions $\delta\theta_{\mathrm{CO},k}(\omega)$, $\delta\theta_{\mathrm{O},k}(\omega)$, and $\delta\theta_{1\times 1,k}(\omega)$ and characterizes the relaxation process, whereas

$$\operatorname{Im}\omega_n(k) = 2\sqrt[6]{\frac{q^2(k)}{4} + |D(k)|}\cos\frac{\operatorname{arctg}\frac{2\sqrt{|D(k)|}}{q(k)}}{3}\times \\ \times\sin\frac{2n\pi}{3} \tag{9}$$

determines the frequency of oscillations.

3. Numerical Solutions

3.1. Homogeneous surface

The system is stable if

$$\mathrm{Re}\,\omega(k) < 0 \tag{10}$$

for all k, i.e. when all normal modes exponentially decrease. If the inequality $\mathrm{Re}\,\omega(k) > 0$ is satisfied at a certain k at least for one mode, the whole system becomes unstable, because the amplitude of the corresponding motion will grow. In the plane of parameters $(\overline{p}_{\mathrm{O}_2}, \overline{p}_{\mathrm{CO}})$, condition (10) determines the stability region for the system (Fig. 1).

As one can see from Fig. 1, there arise four regions in the pressure plane. In regions I, II, and IV, the system is stable, because deviations from the equilibrium exponentially decrease in regions I and IV, and damped oscillations are observed in region II. In region I, the catalytic activity is high, since adsorbed CO molecules and oxygen are observed on the surface. Under those conditions, there is a high probability for the oxidation reaction to run. Region IV, on the contrary, is characterized by a low catalytic activity, because almost the whole catalyst surface is covered with adsorbed CO molecules. A probability for the reaction to run under such conditions is very low. Beyond the boundaries of those regions, one or several normal modes become unstable, and the system spontaneously leaves the initial stationary state (Fig. 2). This is region III in the stability diagram. When the controlling parameter varies, we obtain transitions from one stability mode to another one.

In Fig. 3, the dependences of the real part of the dispersion relation $\mathrm{Re}\,\omega$ on the partial pressure $\overline{p}_{\mathrm{CO}}$ are shown for various wave numbers k and at the partial pressure $\overline{p}_{\mathrm{O}_2} = 0.107$. One can see that $\mathrm{Re}\,\omega > 0$ for the wave number $k = 0$ in the pressure interval $0.056 < \overline{p}_{\mathrm{CO}} < 0.063$, which means that the system with those pressure parameters is unstable. The pressure values $\overline{p}_{\mathrm{CO}} = 0.056$ and $\overline{p}_{\mathrm{CO}} = 0.063$, which correspond to the stability region limits, are critical.

Figure 4 demonstrates the dispersion dependences of $\mathrm{Re}\,\omega$ and $\mathrm{Im}\,\omega$ on the wave number k for the pressures $\overline{p}_{\mathrm{CO}}$ corresponding to different regions in the stability diagram exhibited in Fig. 1 and at the constant values of other parameters. In regions I and

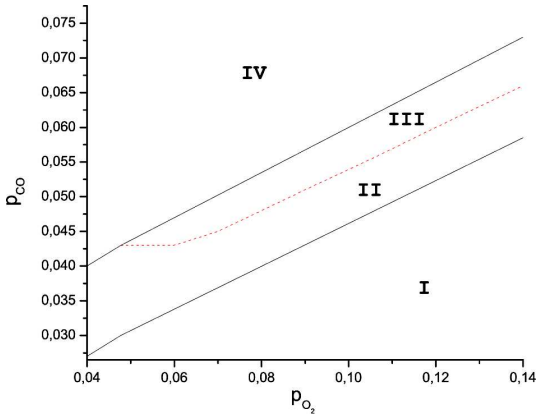

Fig. 1. Diagram of stability in the pressure plane $(\overline{p}_{\mathrm{O}_2}, \overline{p}_{\mathrm{CO}})$. The dashed curve correspond to the condition $\mathrm{Re}\,\omega = 0$. The limit cycle is realized in region III

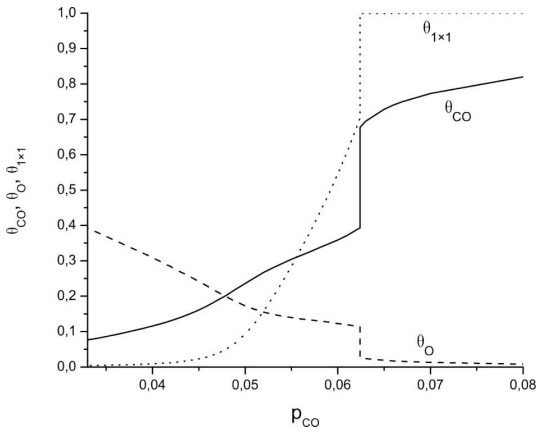

Fig. 2. The stationary state as a function of the pressure $\overline{p}_{\mathrm{CO}}$. At the value of pressure $\overline{p}_{\mathrm{CO}} = 0.0624$, the system undergoes a kinetic phase transition of the first order from the reactive state into an inactive one

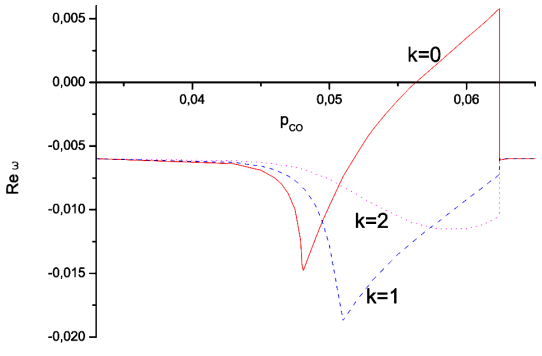

Fig. 3. Real part of the dispersion relation, $\mathrm{Re}\,\omega$, versus the partial pressure $\overline{p}_{\mathrm{CO}}$ for various wave numbers k

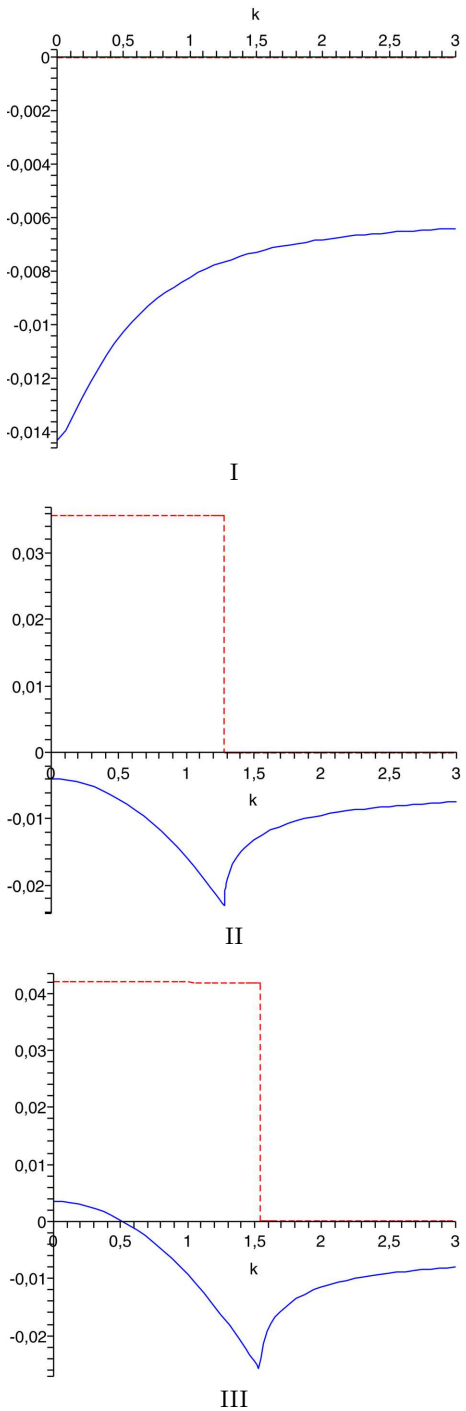

Fig. 4. Dispersion dependences of the real ($\mathrm{Re}\,\omega$, solid curves) and imaginary ($\mathrm{Im}\,\omega/10$, dashed curves) parts of the dispersion relation on the wave vector k at the pressure $\overline{p}_{\mathrm{CO}} = 0.048$ (region I), 0.053 (region II), and 0.06 (region III). The partial pressure of oxygen $\overline{p}_{\mathrm{O}_2} = 0.107$ in all cases

IV, the behaviors of $\mathrm{Re}\,\omega(k)$ and $\mathrm{Im}\,\omega(k)$ are similar; namely, the imaginary part of the dispersion relation $\mathrm{Im}\,\omega = 0$, and the real part $\mathrm{Re}\,\omega < 0$ at any wave number k. Therefore, Fig. 4 demonstrates the results only for regions I, II, and III.

In regions I, II, and IV, the system is stable, because $\mathrm{Re}\,\omega < 0$ for all k. In region III, it is unstable, because $\mathrm{Re}\,\omega > 0$ at $k_0 = 0$. In particular, at the pressure $\overline{p}_{\mathrm{CO}} = 0.06$ in the system with the stationary point ($\theta_{\mathrm{CO}} = 0.359$, $\theta_{\mathrm{O}} = 0.123$, $\theta_{1\times1} = 0.545$), the Hopf bifurcation scenario with $\mathrm{Im}\,\omega(k_0 = 0) = 0.419$ and $\mathrm{Re}\,\omega(k_0 = 0) = 0.0033$ is realized.

The Hopf instability is known [14] to be a local dynamic instability, which arises in a nonlinear system with several time scales and requires that the following conditions should be satisfied: $\mathrm{Im}\,\omega(k_0 = 0) > 0$ and $\mathrm{Re}\,\omega(k_0 = 0) > 0$. It is responsible for the appearance of a new attractor, the limit cycle (a closed orbit), in system's phase space [15]. As a result of the Hopf bifurcation, the system evolves over the states in the limit cycle (self-oscillations).

In this case, the system remains stable with respect to homogeneous fluctuations, because the secular equation (5) at the zero wave number transforms into the equation of the corresponding homogeneous reaction. Therefore, the possibility of self-oscillations in the system can be determined analytically by taking the presence of various time scales into account in the description of the relaxation [16, 17].

Let $\theta_{\mathrm{CO}}(t)$ and $\theta_{\mathrm{O}}(t)$ be rapidly relaxing variables, and $\theta_{1\times1}(t)$ a slow variable. Then, in the time interval $t < \tau_1, \tau_2 \ll \tau_3$, where τ_1, τ_2, and τ_3 are the relaxation times for $\theta_{\mathrm{CO}}(t)$, $\theta_{\mathrm{O}}(t)$, and $\theta_{1\times1}(t)$, respectively, the variation of $\theta_{1\times1}(t)$ is a small quantity: $\mathrm{d}\theta_{1\times1}/\mathrm{d}t \approx 0$. Under this assumption,

$$\frac{\mathrm{d}\theta_{1\times1}}{\mathrm{d}t} = \overline{k}_5 \left(\left[1 + \exp\left(\frac{u_0 - \theta_{\mathrm{CO}}}{\delta u} \right) \right]^{-1} - \theta_{1\times1} \right) \approx 0, \tag{11}$$

which yields

$$\theta_{1\times1} \approx \frac{1}{1 + \exp\left(\frac{u_0 - \theta_{\mathrm{CO}}}{\delta u}\right)}. \tag{12}$$

Substituting this formula into the second equation of system (2), we obtain the following system of two effective chemical kinetics equations for the coverages

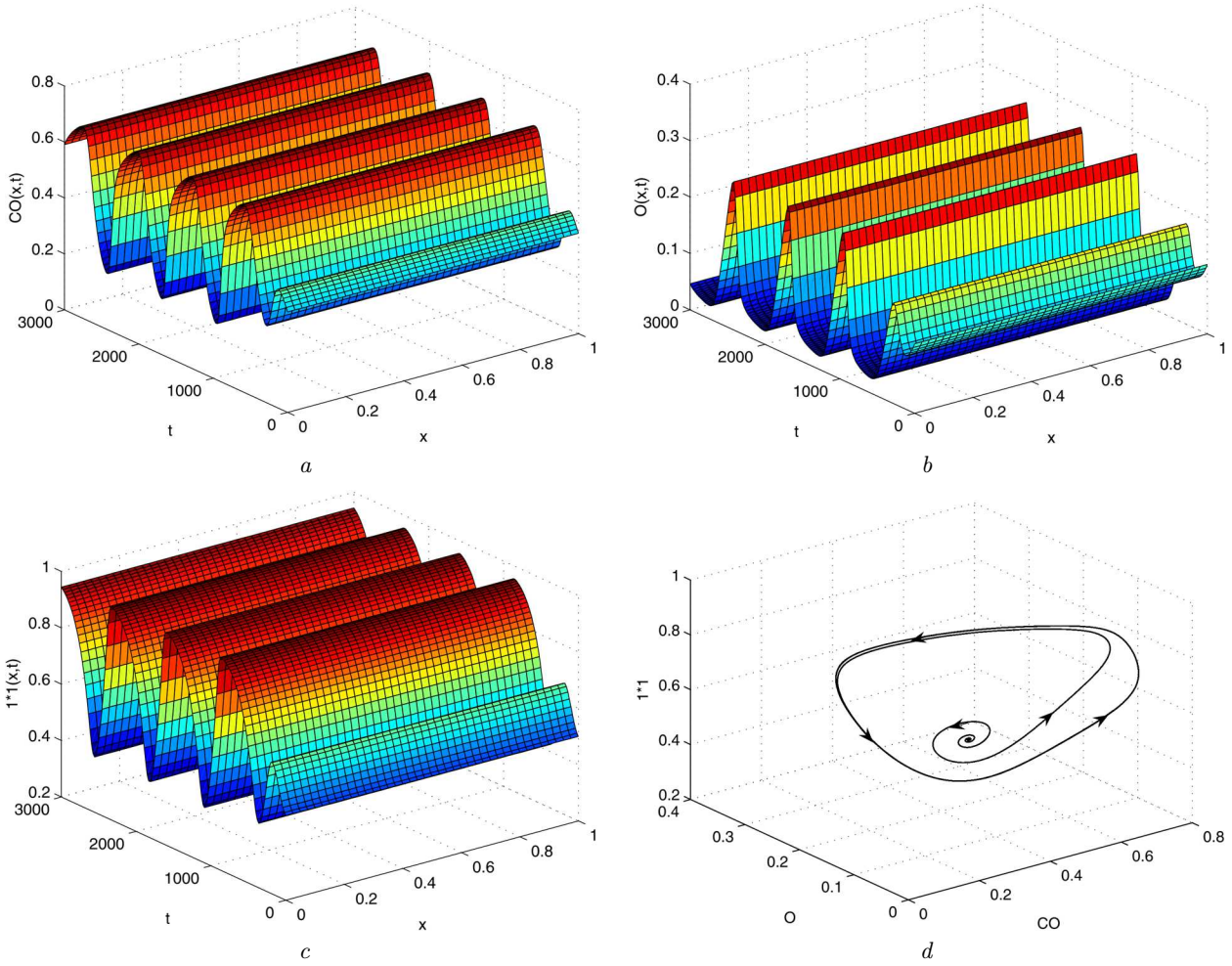

Fig. 5. Self-oscillations of the coverages $\theta_{\mathrm{CO}}(a)$, θ_{O} (b), and the surface geometry $\theta_{1\times1}$ (c) at the pressure $\overline{p}_{\mathrm{CO}} = 0.06$. (d) Phase trajectory of the system in the self-oscillation regime at the pressure $\overline{p}_{\mathrm{CO}} = 0.06$

$\theta_{\mathrm{CO}}(t)$ and $\theta_{\mathrm{O}}(t)$:

$$\begin{aligned}
&\frac{\mathrm{d}\theta_{\mathrm{CO}}}{\mathrm{d}t} = F_{\mathrm{CO}}(\theta_{\mathrm{CO}},\theta_{\mathrm{O}}) = \overline{p}_{\mathrm{CO}}(1-\theta_{\mathrm{CO}}^3) - \\
&-\overline{d}\theta_{\mathrm{CO}} - \theta_{\mathrm{CO}}\theta_{\mathrm{O}}, \\
&\frac{\mathrm{d}\theta_{\mathrm{O}}}{\mathrm{d}t} = F_{\mathrm{O}}(\theta_{\mathrm{CO}},\theta_{\mathrm{O}}) = \\
&= \overline{p}_{\mathrm{O}_2}\left(1+\left[1+\exp\left(\tfrac{u_0-\theta_{\mathrm{CO}}}{\delta u}\right)\right]^{-1}\right)\times \\
&\times(1-\theta_{\mathrm{CO}}-\theta_{\mathrm{O}})^2 - \theta_{\mathrm{CO}}\theta_{\mathrm{O}}.
\end{aligned} \tag{13}$$

In the general case of a system of two autonomous equations $\dot{X}_1 = F^{(1)}(X_1, X_2)$ and $\dot{X}_2 = F^{(2)}(X_1, X_2)$, the stationary point generating a limit cycle becomes unstable under the condition $\mathrm{Re}\,\Phi < 0$, where $\mathrm{Re}\,\Phi$ is the real part of the Floquet exponent. As a result, the condition for the limit cycle to arise can be written in the form [16]

$$\mathrm{Re}\,\Phi = \frac{1}{8}\left(F^{(1)}_{111} + F^{(1)}_{122}\right) + \left(F^{(2)}_{222} + F^{(2)}_{112}\right) < 0, \tag{14}$$

where

$$F^{(\delta)}_{\alpha\beta\gamma} \equiv \left.\frac{\partial^3 F^{(\delta)}}{\partial X_\alpha \partial X_\beta \partial X_\gamma}\right|_{\mathbf{X}=\mathbf{X}^s} \quad \text{for } \alpha,\beta,\gamma,\delta = 1,2.$$

In our case, contributions from $F_{\mathrm{CO}}(\theta_{\mathrm{CO}},\theta_{\mathrm{O}})$ (of the type $F^{(1)}_{111}$) can arise if $F_{\mathrm{CO}}(\theta_{\mathrm{CO}},\theta_{\mathrm{O}})$ contains a nonlinearity of the third or higher order. Contribu-

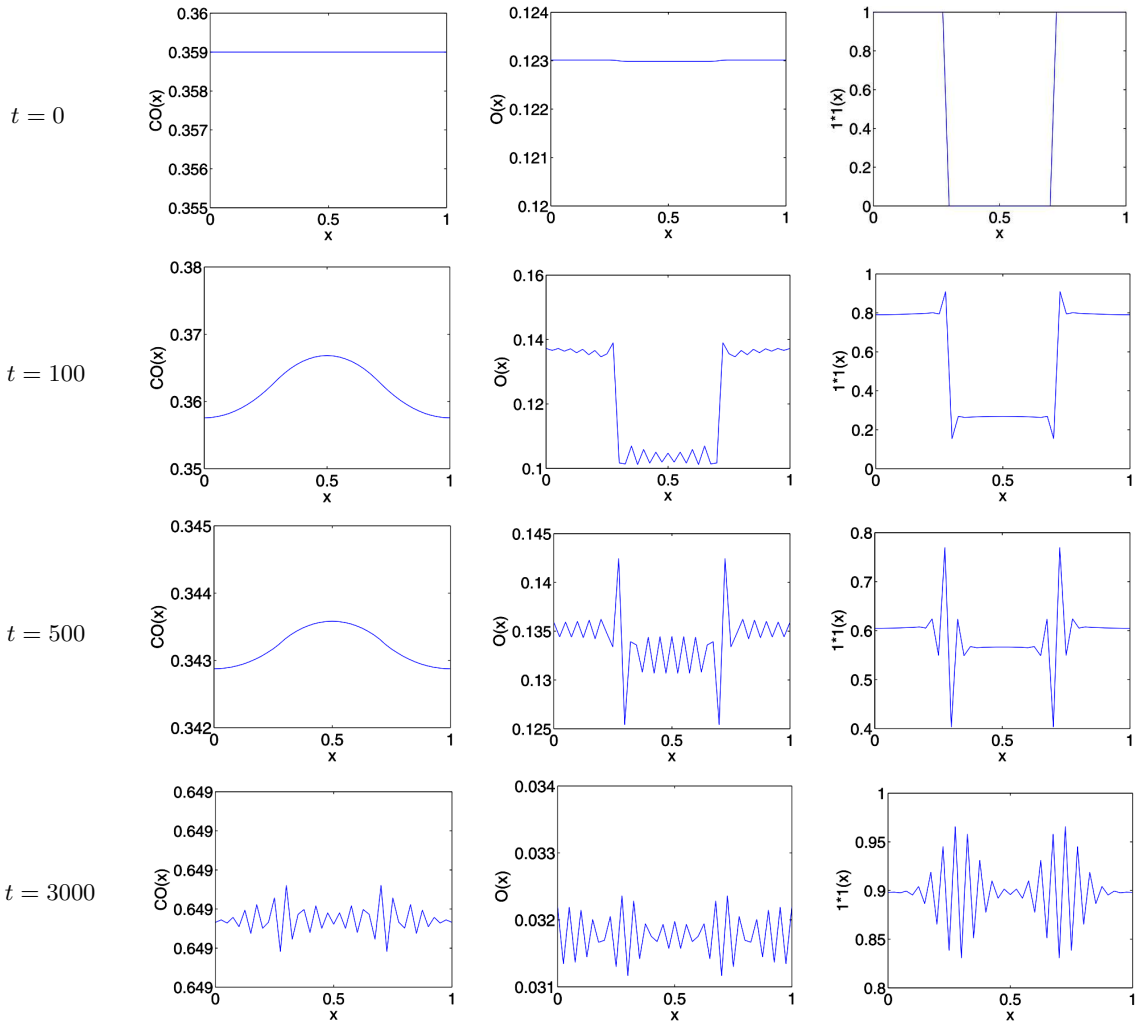

Fig. 6. Evolution of the spatial distributions of the coverages θ_{CO} (left column), θ_{O} (central column), and the surface geometry $\theta_{1\times1}$ (right column)

tions from $F_{\mathrm{O}}(\theta_{\mathrm{CO}},\theta_{\mathrm{O}})$ (of the type $F^{(2)}_{112}$) appear owing to the nonlinear dependence $\theta_{1\times1}=f(\theta_{\mathrm{CO}})$. For the system of equations (13), a condition for the emergence of limit cycle looks like

$$-3\overline{p}_{\mathrm{CO}}+\frac{\overline{p}_{\mathrm{O_2}}}{\delta u}\frac{\exp\left(\frac{u_0-\theta^s_{\mathrm{CO}}}{\delta u}\right)}{\left(1+\exp\left(\frac{u_0-\theta^s_{\mathrm{CO}}}{\delta u}\right)\right)^2}\times$$
$$\times\left(-\frac{1}{\delta u}\tanh\left(\frac{u_0-\theta^s_{\mathrm{CO}}}{2\delta u}\right)(1-\theta^s_{\mathrm{CO}}-\theta^s_{\mathrm{O}})+2\right)<0. \tag{15}$$

On the basis of the Hopf theory, it is possible to determine the dependence of the limit cycle period, which corresponds to stable self-oscillations of the dynamic variables in the system, on an external parameter. The oscillation period $T=2\pi/\mathrm{Im}\,\omega(k_0=0)$. For the system under consideration, the oscillation period equals

$$T=\pi\left(\sqrt[6]{\frac{q^2(k_0)}{4}+|D(k_0)|}\times\right.$$
$$\left.\times\cos\left(\frac{1}{3}\,\mathrm{arctg}\,\frac{2\sqrt{|D(k_0)|}}{q(k_0)}\right)\times\sin\frac{2\pi}{3}\right)^{-1}.$$

Self-oscillations of the coverages θ_{CO}, θ_{O} and the surface geometry $\theta_{1\times1}$, as well as the corresponding phase trajectory of the system, are shown in

Fig. 5. One can see that the phase trajectory is twisted on a closed curve, which is the limit cycle. In other words, the average adsorbate coverages and the fraction of the 1×1 surface undergo periodic oscillations, which is a result of the Hopf bifurcation.

3.2. Inhomogeneous surface

In order to study inhomogeneities on the surface, let us consider a one-dimensional case of the Pt(110) surface with various surface phases: the reconstructed 1×2 phase around the center and the non-reconstructed 1×1 phase near the boundaries. The surface size is $L_x = 1$ μm. Periodic boundary conditions correspond to the absence of fluxes across the boundaries of the interval $0 < x < 1$. Initial conditions are selected as a local perturbation of the dynamic variable $\theta_{1\times1}$ around the interval center [7]:

$$\theta_{1\times1}(x, t = 0) = \begin{cases} 1, & x < 0.3 \text{ and } x > 0.7, \\ 0, & 0.3 < x < 0.7. \end{cases} \qquad (16)$$

All other spatial points are in a stationary state. The reaction and diffusion parameters are selected to correspond to the self-oscillation mode. In other words, if the whole substrate surface had a homogeneous structure, the evolution of the system would be characterized by uniform periodic oscillations of the coverages $\theta_{\mathrm{CO}}(x,t) = \theta_{\mathrm{CO}}(t)$, $\theta_{\mathrm{O}}(x,t) = \theta_{\mathrm{O}}(t)$, and the surface fraction $\theta_{1\times1}(x,t) = \theta_{1\times1}(t)$, as is shown in Fig. 5. In the case when the reconstructed 1×2 phase is located inside the non-reconstructed 1×1 phase, the gradient of the surface coverage near the $1 \times 2/1 \times 1$ phase interface results in the transition into an inhomogeneous state. Figure 6 demonstrates the spatial distributions of the coverages θ_{CO}, θ_{O}, and the surface geometry $\theta_{1\times1}$ at the time moments $t = 0$, 100, 500, and 3000. They illustrate the evolution of a new inhomogeneous surface state. In this state, the spatial distribution of the coverage θ_{CO} weakly depends on the surface structure. This dependence looks like a peak around the specimen center, but the peak becomes almost unobservable in the course of time. The coverage of adsorbed oxygen is more sensitive to the surface structure at the initial time moment. As the time grows, an inhomogeneous distribution of oxygen with an oscillatory character is established on the surface. At initial stages of evolution, $\theta_{\mathrm{O}}(x)$-oscillations are more pronounced around the specimen center, but ultimately they extend over the whole surface. The

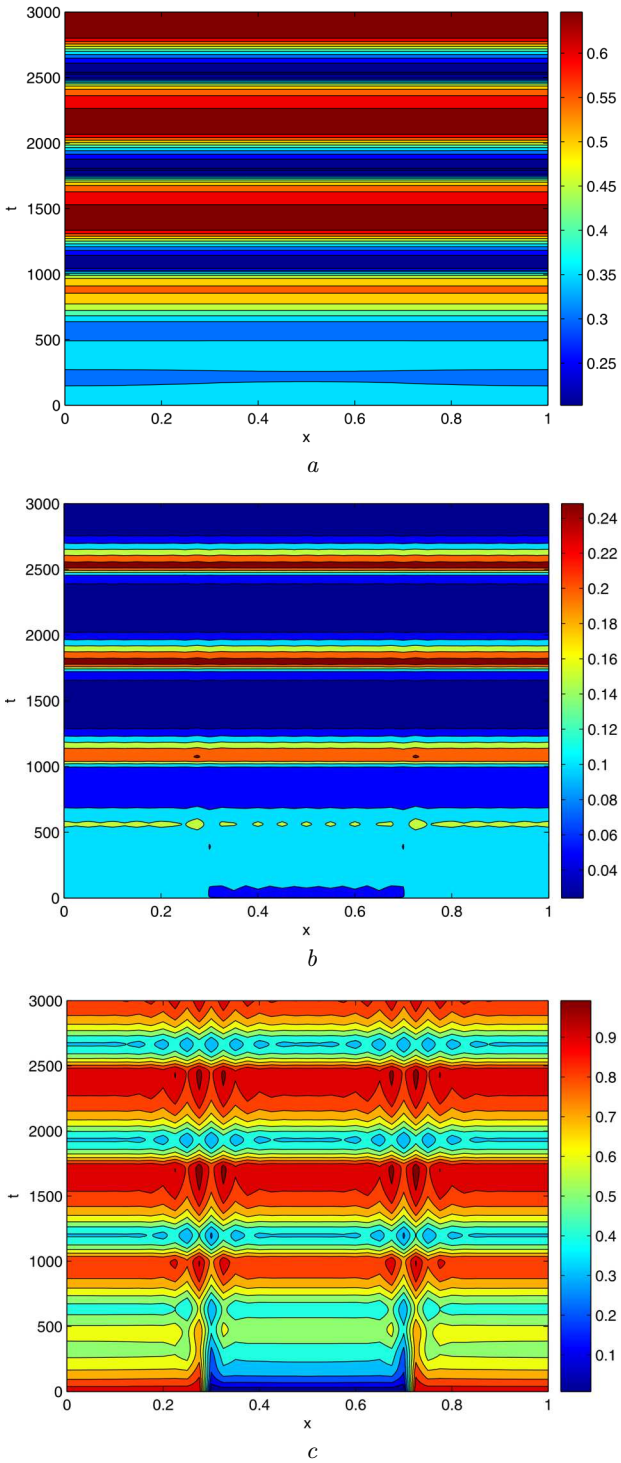

Fig. 7. Amplitude maps of self-oscillations of the coverages θ_{CO}, θ_{O}, and the surface geometry $\theta_{1\times1}$ at the pressure $\overline{p}_{\mathrm{CO}} = 0.06$

surface structure also remains inhomogeneous, with a neatly expressed oscillatory spatial distribution.

The emergence of spatial inhomogeneities results in the wave front deformation. In Fig. 7, the self-oscillation regime of the system at the pressure $\overline{p}_{\rm CO} = 0.06$ is shown in the form of amplitude maps. The self-oscillations are depicted by varying the color (intensity) of their background. One can observe the appearance of spatio-temporal patterns, which are insignificant by magnitude for the coverage $\theta_{\rm O}$, but are strongly pronounced for the surface fraction $\theta_{1\times1}$. The distribution of $\theta_{\rm CO}$ is almost homogeneous in space and independent of the surface geometry.

4. Conclusions

A dispersion relation for the reaction-diffusion model of the catalytic carbon monoxide oxidation is obtained. The imaginary part of the relation is responsible for oscillatory solutions, and the real one describes the stability of the solution and is responsible for the relaxation.

An oscillation regime of the limit-cycle type (result of the Hopf bifurcation) is revealed in a narrow region of the phase diagram between two homogeneous stable states corresponding to a high and low catalytic activities. The period of stable self-oscillations of the dynamical variables of the system is determined.

Surface inhomogeneities are analyzed by considering a one-dimensional Pt(110) surface with two surface phases: a reconstructed 1×2 phase at the specimen center and a non-reconstructed 1×1 phase near the specimen boundaries. Some spatio-temporal patterns are revealed. They turn out insignificant for the coverage $\theta_{\rm O}$ and are strongly pronounced for the surface fraction $\theta_{1\times1}$. The distribution of $\theta_{\rm CO}$ turned out almost homogeneous in space and independent of the surface geometry.

1. M. Bar, S. Nettesheim, H.H. Rotermund, M. Eiswirth, and G. Ertl, Phys. Rev. Lett. **74**, 1246 (1995).
2. K.C. Rose, D. Battogtokh, A. Mikhailov, R. Imbihl, W. Engel, and A.M. Bradshaw, Phys. Rev. Lett. **76**, 3582 (1996).
3. A. von Oertzen, H.H. Rotermund, A.S. Mikhailov, and G. Ertl, J. Phys. Chem. B **104**, 3155 (2000).
4. V.V. Gorodetskii and W. Drachsel, Appl. Cat. A **188**, 267 (1999).
5. A.M. Zhabotinsky and A.N. Zaikin, Nature **255**, 535 (1970).
6. V.K. Vanag, Physics-Uspekhi (Advances in Physical Sciences) **174**, 991 (2004) (in Russian).
7. N. Pavlenko, Phys. Rev. E **77**, 026203 (2008).
8. R.B. Hoyle, A.T. Anghel, M.R.E. Proctor, and D.A. King, Phys. Rev. Lett. **98**, 226102 (2007).
9. J. Verdasca, P. Borckmans, and G. Dewel, Phys. Rev. E **64**, 055202 (2001).
10. H. Levine and X. Zou, Phys. Rev. E **48**, 50 (1992).
11. O.I. Gichan, L.B. Lerman, L.G. Grechko, and Yu.P. Sklyarov, Bulletin of Kiev university. Series: Physics & Mathematics **1**, 311 (2005) (in Ukrainian).
12. I.S. Bzovska and I.M. Mryglod, Condens. Matter Phys. **13**, 34801 (2010).
13. M. Bertram and A.S. Mikhailov, Phys. Rev. E **67**, 036207 (2003).
14. O.I. Gichan and L.G. Grechko, Bulletin of University of Kyiv. Series: Physics & Mathematics **4**, 311 (2007) (in Ukrainian).
15. W. Ebeling, *Patterns Formation in Irreversible Processes* (Moscow–Izhevsk, 2004) (in Russian).
16. A.I. Olemskoi and I.A. Shuda, *Statistical Theory of Self-Organized Complex Systems* (Sumy Univ. Publ. House, Sumy, 2010) (in Russian).
17. I.S. Bzovska and I.M. Mryglod, Preprint ICMP-12-14U (Institute for Condensed Matter Physics, Lviv, 2012) (in Ukrainian).

Received 22.05.15.
Translated from Ukrainian by O.I. Voitenko

І.С. Бзовська, І.М. Мриглод

ПОВЕРХНЕВІ СТРУКТУРИ В КАТАЛІТИЧНІЙ РЕАКЦІЇ ОКИСЛЕННЯ МОНООКСИДУ ВУГЛЕЦЮ

Р е з ю м е

Роботу присвячено дослідженню механізму виникнення поверхневих просторово-часових структур під час протікання каталітичної реакції окислення монооксиду вуглецю на поверхні Pt(110), яка може містити структурно відмінні ділянки, що утворюються під час CO-індукованого переходу від реконструйованої 1×2 фази до об'ємної 1×1 фази. Аналіз нестійкостей у часі і просторі системи проведено на основі методів лінійної теорії стійкості та чисельного моделювання. Показано, що на неоднорідній поверхні при певних параметрах в системі виникають просторово-часові поверхневі структури для покриття киснем та частки поверхні структури 1×1. Розподіл покриття монооксидом вуглецю є майже однорідним у просторі та незалежним від геометрії поверхні.